0026-895X/99/020386-10$3.00/0

MOLECULAR PHARMACOLOGY, **55:**386–395 (1999).

The Startle Disease Mutation Q266H, in the Second Transmembrane Domain of the Human Glycine Receptor, Impairs Channel Gating

ANDREW J. MOORHOUSE, PATRICE JACQUES, PETER H. BARRY, and PETER R. SCHOFIELD

School of Physiology and Pharmacology, University of New South Wales, Sydney, Australia (A.J.M., P.H.B.) and The Garvan Institute of Medical Research, Darlinghurst, Sydney, Australia (P.J., P.R.S.)

Received, July 27, 1998; accepted November 3, 1998

This paper is available online at http://www.molpharm.org

ABSTRACT

Hyperekplexia (startle disease) results from mutations in the glycine receptor chloride channel that disrupt inhibitory synaptic transmission. The Q266H missense mutation is the only hyperekplexia mutation located in the transmembrane domains of the receptor. Using recombinant expression and patch-clamping techniques, we have investigated the functional properties of this mutation. The ability of glycine and taurine to open the channel was reduced in the mutated channel, as shown by a 6-fold shift in the concentration-response curve for both agonists. This was not accompanied by similar changes in agonist displacement of strychnine binding, suggesting that the mutation affects functions subsequent to ligand binding. Taurine was also converted to a weak partial agonist and antagonized the actions of glycine, consistent with changes in its channel gating efficacy. Because the Q266H mutation is within the pore-forming second transmembrane domain, we tested for a direct interaction with permeating ions. No change in either the cation/anion selectivity ratio or in single channel conductance levels was observed. No differential effects of Zn^{++}, pH, and diethylpyrocarbonate were observed, implying that the histidine side chain is not exposed to the channel lumen. Single-channel recordings revealed a significant reduction in open times in the mutant receptors, at both high and low agonist concentrations, consistent with the open state of the channel being less stable. This study demonstrates that residues within the second transmembrane domain of ligand-gated ion channel receptors, even those whose side chains do not directly interact with permeating ions, can affect the kinetics of channel gating.

The glycine receptor (GlyR) is a member of the ligand-gated ion channel (LGIC) superfamily and plays an important role in the central processing of sensory and motor information (reviews in Schofield et al., 1996; Zafra et al., 1997). Mutations within the gene encoding the α1 subunit of the human GlyR (GLRA1) are causative for a rare neurological disease known as startle disease or hereditary hyperekplexia (Shiang et al., 1993; 1995; Rees et al., 1994; Brune et al., 1996; Elmslie et al., 1996; Milani et al., 1996). This disease is characterized by symptoms resembling the hyperexcitability generated by sublethal poisoning with the convulsant GlyR antagonist strychnine (reviewed in Floeter and Hallet, 1993). Investigation of the molecular defects that result in hyperekplexia has given insights into the structure-function relationships of LGICs. These receptor channels, whose members include the nicotinic acetylcholine receptor (nAChR), the γ-aminobutyric acid type A ($GABA_A$) receptor, and the 5-hydroxytryptamine type 3 receptor, are pentameric proteins whose α subunits consist of large ligand binding extracellular domains connected to four membrane spanning domains (M1 to M4), the second of which is thought to contribute to the channel pore (Bertrand et al., 1993; Akabas et al., 1994).

All of the hyperekplexia mutations studied to date cause single-point substitution of residues in either the short intracellular (M1-M2) or extracellular (M2-M3) loops that flank the luminal M2 domain. The most frequently observed mutation results in either an uncharged leucine or glutamine being substituted for a charged arginine residue at the extracellular border of the M2 region (R271L, R271Q; Shiang et al., 1993). When α1-homomeric GlyRs containing these two hyperekplexia mutations were expressed in human embryonic kidney 293 (HEK-293) cells, a dramatic decrease in the magnitude of glycine activated currents was observed, which was due to both a decrease in sensitivity of the receptors to glycine and a redistribution of the single channel's conductance states to lower levels. This decrease in current magni-

Supported by the National Health and Medical Research Council of Australia.

ABBREVIATIONS: GlyR, glycine receptor; n_H, Hill coefficient; HEK-293, human embryonic kidney 293 cell line; LGIC, ligand-gated ion channel; WT, wild type; M2, second transmembrane domain; nAChR, nicotinic acetylcholine receptor; $GABA_AR$, γ-aminobutyric acid type A receptor.

tude had been corrected for any changes in the number of receptors expressed on the cell surface and was observed in the absence of any change in the sensitivity of glycine currents to strychnine (Rajendra et al., 1994; Langosch et al., 1994). In addition, these mutations converted the agonists β-alanine and taurine to competitive antagonists, and the competitive antagonist picrotoxin to an allosteric potentiator and noncompetitive antagonist (Lynch et al., 1995; Rajendra et al., 1995). These results suggest that the Arg271 residue is crucial for transducing the allosteric coupling from ligand binding to channel activation.

The subsequent investigation of a number of less common missense mutations in the α1 subunit that also cause hyperekplexia, identified additional residues involved in this gating process. These mutations include the recessive I244A mutation at the intracellular border of the M2 domain (Rees et al.,1994) and the dominant K276E and Y279C mutations, both located within the M2 to M3 extracellular loop (Shiang et al., 1995; Elmslie et al., 1996). GlyRs containing these mutations displayed properties similar to the R271L and R271Q mutations; that is, a decrease in glycine sensitivity and a change in agonist/antagonist transduction for taurine and β-alanine (Lynch et al., 1997). In addition, the functional consequences of the K276E mutation could be interpreted solely in terms of an impairment of channel gating kinetics without effects on ligand binding or conductance (Lewis et al., 1998). The position of these hyperekplexia mutations, coupled with similar phenotypes observed for adjacent alanine-mutated residues suggested that the M1 to M2 and the M2 to M3 loops act as hinges to gate the M2 domains during channel opening (Lynch et al., 1997). This postulate is also consistent with the kinked rotation model proposed by Unwin (1995) on the basis of electron micrographic evidence.

The only hyperekplexia mutation which predicts a missense mutation to a residue that is not located in either of the M1 to M2 or the M2 to M3 loops is the substitution of a glutamine by a histidine at residue 266 (Q266H), approximately two thirds of the way into the M2 domain (Milani et al., 1996). In this paper, we describe the properties of recombinant human α1 homomeric GlyRs containing the Q266H hyperekplexia mutation.

Materials and Methods

Mutagenesis and Expression. The α1 subunit cDNA of the human GlyR and human CD4 antigen cDNA were subcloned into the pCIS2 and pRc/CMV expression vectors, respectively, both of which contain the human cytomegalovirus promoter-enhancer. HEK-293 cells were transiently cotransfected with these constructs at a ratio of 10:1 with the calcium phosphate precipitate method (Chen and Okayama, 1987). Mutations to human GlyR α1 cDNA were constructed in the pCIS2 expression vector with oligonucleotide-directed polymerase chain reaction mutagenesis and were confirmed by sequencing the cDNA clones. Patch clamp and radioligand-binding studies were conducted 36 to 96 h after transfection. Just before patch clamp recordings, coverslips containing transfected HEK-293 cells were gently washed with bath solution containing magnetic polystyrene microspheres coated with anti-CD4 antibody (ratio ≈ 1:2500; Dynabeads M-450 CD4; Dynal, Oslo, Norway). Typically, one or two good recordings were obtained in each transfection.

Drugs and Solutions. The composition of the bathing solution was as follows: 140 mM NaCl, 10 mM glucose, 5 mM KCl, 2 mM $CaCl_2$, 2 mM $MgCl_2$, 10 mM HEPES, and ≈6 mM NaOH, pH 7.4. For dilution potential experiments, 75 mM NaCl was replaced by 136 mM sucrose, an iso-osmotic concentration of sucrose. For assessing the effects of pH, HEPES buffer was replaced with equimolar piperazine-N-N′-bis(2-ethanesulfonic acid) (pH 6.4) or Tris (pH 8.4). Fresh stocks of glycine, taurine, and strychnine were prepared daily and diluted to final concentrations with bath solution. Diethylpyrocarbonate (DEPC) was diluted to the appropriate working concentration in extracellular solution immediately before use. Drugs were applied with a manually controlled multitube perfusion system which gave exchange times of 20 to 80 ms (as judged by the time course of the change in open pipette current upon perfusion with diluted bath solution). The pipette solution contained: 145 mM CsCl, 2 mM $CaCl_2$, 2 mM $MgCl_2$, 10 mM HEPES, 10 mM EGTA, and ≈29 mM CsOH, pH 7.3. All drugs and chemicals were purchased from Sigma Chemical Co. (St. Louis, MO).

Electrophysiology. Glycine-gated currents were measured at room temperature (≈22°C) with the whole cell or excised outside-out patch clamp recording techniques. Round and bipolar single cells lightly labeled with Dynabeads were generally chosen for electrophysiological recordings. Patch pipettes were pulled from capillary tubing (Vitrex, Herlev, Denmark), coated with Sylgard 184 (Dow Corning, Midland, MI), and fire-polished just before use. They had resistances of 2 to 8 MΩ when filled with pipette solution. Data were recorded to disk with an Axopatch 1D amplifier and pClamp 6 acquisition software (Axon Instruments, Foster City, CA). Whole-cell recordings were filtered at 500 Hz (−3 dB frequency) before being digitized at 2000 Hz with a TL-1 interface (Axon Instruments). The empirical Hill equation, fitted to data from individual experiments by a nonlinear least-squares algorithm (Sigmaplot for Windows ver. 4; Jandel Scientific, Corte Madera, CA), was used to calculate the maximum current amplitude, 50% concentration for activation (EC_{50}) and inhibition (IC_{50}), and Hill coefficients (n_H). All voltages have been corrected for liquid junction potentials with the program JPCalc (Barry, 1994; contact P.H.B. for program availability).

All single channel recordings were obtained with the outside-out configuration of the patch clamp technique at a membrane potential of −60 mV. Single-channel data were digitized directly onto the hard disk of a Pentium computer at 10 kHz, after filtering at 2 kHz with a 4-pole Bessel filter supplied with the patch clamp amplifier. Single-channel conductances were measured, both directly and by fitting gaussian distributions to amplitude histograms, before kinetic analysis. All single-channel analysis used pClamp 6 software. Amplitude histograms had bin widths from 0.05 to 0.20 pA. Open and closed time distributions were constructed from event lists generated with a 50% threshold criteria, chosen in general to be 50% of the main conductance level. On occasions when there were clear contributions from a subconductance level, event lists were constructed with multiple conductance levels. In these situations, only the open and closed time distributions of the main conductance state were further analyzed. Only events that were within about 2 S.D.s from the averaged main conductance level and were longer than three times the rise time of the filter (cutoff 0.2 ms) were accepted for futher analysis. Events that had amplitudes greater than the amplitude of the main conductance level (i.e., multiple openings) were also excluded from the analysis. Open and closed times were binned logarithmically with seven or eight bins per decade and plotted against the square root of their frequency. Time constants describing the distribution of binned closed and open times were obtained from fitting exponential functions to these distributions with a least-squares optimization procedure.

All data are presented as mean ± S.E.M. Statistical significance was assessed with Student's t test at a probability level of 0.05.

[^{3}H]Strychnine-Binding Assays. Transfected cells were incubated with [^{3}H]strychnine (1–50 nM; 23 Ci/mmol; New England Nuclear, Boston, MA) with and without 10 μM cold strychnine to determine nonspecific binding. After incubation to equilibrium at 4°C for 60 min, cells were collected by rapid filtration onto Whatman GF/B filter paper and the amount of [^{3}H]strychnine remaining bound was determined. The K_d and B_{max} for the [^{3}H]strychnine saturation

isotherms and the K_i for glycine and taurine displacement of bound [^{3}H]strychnine were estimated by nonlinear regression with the Inplot and Prism programs, respectively (GraphPad Software, San Diego, CA). These values were determined in triplicate for each binding isotherm and three separate experiments were done measuring B_{max}, K_d, and K_i values in each.

Results

Activation of Wild-Type (WT) and Q266H GlyRs by Glycine. Glycine- gated currents were observed in HEK-293 cells transfected with either WT or Q266H GlyRs (Fig. 1A and B). Application of glycine to cells expressing WT GlyRs induced concentration-dependent inward currents, when held at negative membrane potentials, with an EC_{50} of 22.7 ± 9.7 μM and a n_H of 3.5 ± 0.9 (n = 5). In cells expressing Q266H GlyRs, there was a significant 6-fold shift to the right of the glycine concentration-response curve (EC_{50} = 138.2 ± 31.1 μM, p = .02) without any significant change in the shape of the curve [n_H =2.5 ± 0.3 (n = 10), Fig. 1C]. In cells in which ≥85% series resistance compensation was used, the maximum apparent peak whole-cell conductance of both receptor types was similar but quite variable, being 10.7 ± 3.9 nS/pF (n = 12) for the WT GlyRs and 9.7 ± 6.2 nS/pF (n = 13) for the Q266H GlyRs. Despite the apparent difference in Fig. 1, A and B, there was no large or consistent difference in the time course and extent of decay of the glycine-activated currents between WT and Q266H GlyRs (compare also Figs 2A and 4A with 2B and 4B), which in our experimental conditions, is due to a combination of both slow components of desensitization and a redistribution of the transmembrane Cl^- concentration (unpublished observations).

Activation and Inhibition of WT and Q266H GlyRs by Taurine. In α1-homomeric WT GlyRs, the amino acid taurine acts as a full agonist. However, in GlyRs carrying the various hyperekplexia mutations, taurine acts either as a partial agonist or as a competitive antagonist (Rajendra et al., 1995; Lynch et al., 1997). In the present study, taurine activated WT GlyRs to a similar degree as glycine (87 ± 5.2% of maximum glycine response, n = 4) with an EC_{50} and n_H of 280 ± 129 μM and 1.8 ± 0.2, respectively (n = 3; Fig. 2, A and

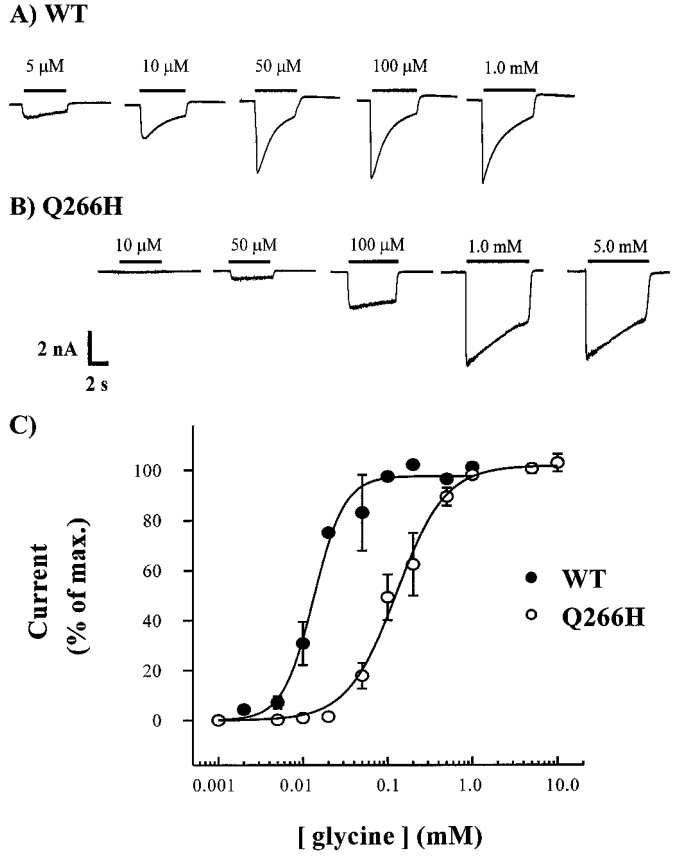

Fig. 1. Examples of whole-cell currents in response to increasing concentrations of glycine, from a HEK-293 cell expressing WT (A) or Q266H (B) GlyRs, in symmetrical Cl^- solutions. Membrane potential was −41 mV. C, mean normalized concentration-response curves for the peak glycine-activated currents in cells expressing WT (●, n = 5) or Q266H (○, n = 10) GlyRs. Error bars represent S.E.M., whereas the continuous lines represent the Hill fits to the mean data. At least six concentrations of agonist were applied in each experiment.

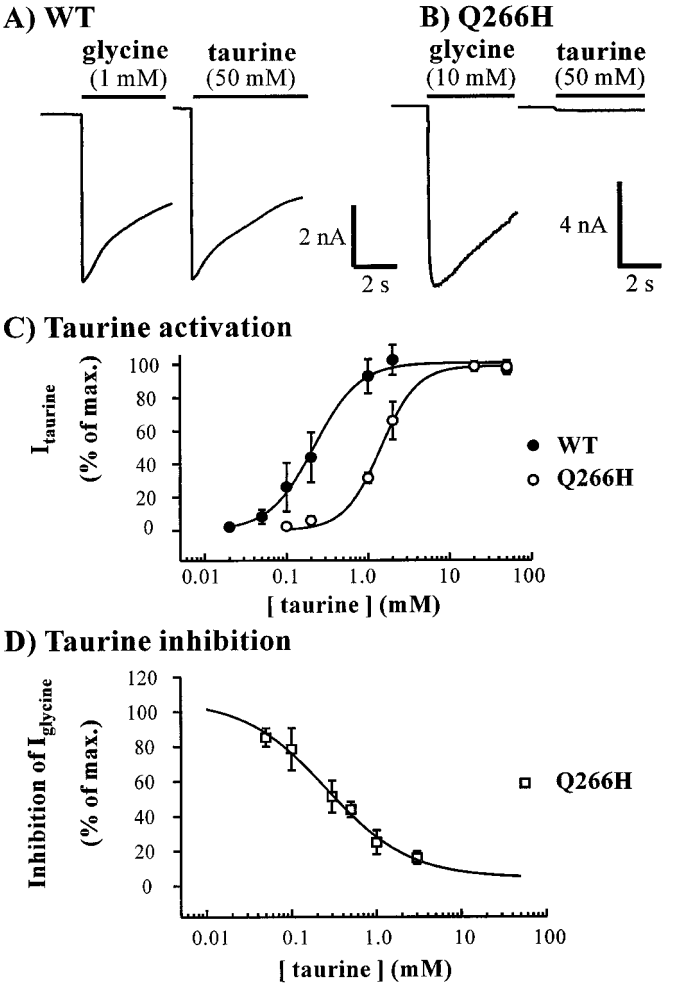

Fig. 2. A comparison of the actions of taurine on WT (A) and Q266H (B) GlyR whole-cell currents in symmetrical Cl^- solutions. In WT GlyRs, taurine and glycine elicit comparable currents. In Q266H GlyRs, however, the maximal taurine current is less than 5% of that elicited by glycine. For each case, glycine and taurine currents were elicited in the same cell at a holding potential of −41 mV. C, activation curves for taurine. The dose-response curve for taurine activation of Q266H GlyRs (○, n = 4) is right-shifted and parallel to that for taurine activation of WT GlyRs (●, n = 3). D, dose-response curve for the mean inhibition of glycine-gated whole-cell currents in Q266H GlyRs induced by coapplication of glycine (10 mM) and taurine (n = 3). The inhibition is expressed as a percentage of the maximum inhibition obtained from Hill fits to the data from individual experiments. C and D, the lines represent Hill plots fitted to the mean data.

C). In contrast, in Q266H GlyRs the maximum taurine currents were much smaller, being only 2.8 ± 0.7% (n = 5) of the maximum glycine activated currents (Fig. 2B). In addition, the EC_{50} for taurine activation was increased 6-fold to 1620 ± 250 μM ($p < .01$) with no significant change in the n_H [2.4 ± 0.8 (n = 4); Fig 2C].

The significantly reduced taurine-activated currents in the Q266H GlyRs, when compared with WT GlyRs, indicated that the mutation may radically alter the efficacy of channel gating in response to this agonist and convert it into a partial agonist. In agreement, coapplication of taurine and glycine elicited smaller currents through Q266H GlyRs than those evoked by application of glycine alone (not shown). In three experiments, coapplication of 50 μM to 3.0 mM taurine along with 10 mM glycine reduced the current activated by glycine alone. The extent of this inhibition was dependent on the taurine concentration (Fig. 2D); Hill fits indicated that the maximum inhibition was 49.0 ± 17.8%. The IC_{50} for this inhibition was 274.9 ± 91.9 μM with an n_H of 0.99 ± 0.12.

[^{3}H]Strychnine-Binding Assays. To investigate the nature of the changes in the agonist responses, we examined the binding of [^{3}H]strychnine to cells expressing WT and Q266H GlyRs and the displacement of this binding by glycine and taurine (Fig 3). There was no difference in the average number of receptor-binding sites expressed per cell, with B_{max} values being 8.20 ± 0.20 × 10^5 (n = 3) for WT GlyRs and 8.50 ± 0.03 × 10^5 (n = 3) for Q266H GlyRs. There was also no difference in the affinity for [^{3}H]strychnine, with K_d values being 10.4 ± 2.4 nM (n = 3) for WT GlyRs and 11.5 ± 0.9 nM (n = 3) for Q266H GlyRs, suggesting no major structural change to the ligand-binding site(s). There was, however, a significant 2-fold reduction in the ability of glycine to displace bound [^{3}H]strychnine, with K_i values of 130 ± 17 μM (n = 5) and 281 ± 31 μM (n = 3) for WT and Q266H GlyRs, respectively. There was also a similar approximate 2-fold reduction in the ability of taurine to displace bound [^{3}H]strychnine [K_i values of 161 ± 44 μM (n = 5) and 367 ± 91 μM (n = 3) for WT and Q266H GlyRs, respectively], although this difference was not statistically significant. These results suggest that the Q266H mutation manifests itself by an apparent slight decrease in the measured ligand binding affinity but also shows that such changes are small and are not likely to explain the full effects of the Q266H mutation on the agonist concentration-response curves or the marked decrease in the maximum taurine response.

Single-Channel Properties. To further study the nature of the changes in the glycine concentration-response curve, and to investigate whether the Q266H mutation also affected the permeation properties of GlyRs, we recorded unitary step changes in current through excised outside-out membrane patches in response to glycine. Low concentrations of glycine (0.1–5.0 μM) elicited clear single-channel openings in patches containing WT GlyRs as illustrated in Fig. 4,A and E. The distribution of these single channel amplitudes revealed multiple conductance levels, about eight levels in all, although in any single patch only three to six different subconductance levels were generally observed (Fig. 4A). The most commonly observed levels (apparent in eight of nine patches) had conductances of ≈95 pS and ≈36 pS, although in any of the eight single patches, the large ≈95 pS conductance level was typically the most frequently observed. The distribution of WT conductance levels and their corresponding incidence and relative contribution are summarized in Table 1. Similarly, in patches containing Q266H GlyRs, low concentrations of glycine (1.0–10 μM) activated single-channel currents of varying conductance (Fig. 4, B and F). These conductances could also be roughly grouped into the same eight subconductance levels seen in the WT GlyRs (Table 1), although once again not all conductances were seen in each patch (two to seven different conductances were generally seen in any one patch). The ≈95 pS conductance level, most prominent in WT GlyRs, was also seen in each of the seven patches of Q266H GlyRs, and typically was the most frequently observed conductance level in these patches (Table 1). It is concluded that there was no difference in the single-channel conductance levels, or in their incidence and relative contribution, between WT and mutant GlyRs.

In contrast to the lack of effect of the Q266H mutation on single-channel conductance levels, it was apparent that mutant receptor single-channel openings, at a variety of agonist concentrations, were briefer and more flickery (compare Fig. 4 A and B; E and F). In an attempt to quantify this observation, dwell-time histograms were constructed from patches containing WT GlyRs (n = 7) and Q266H GlyRs (n = 4). In

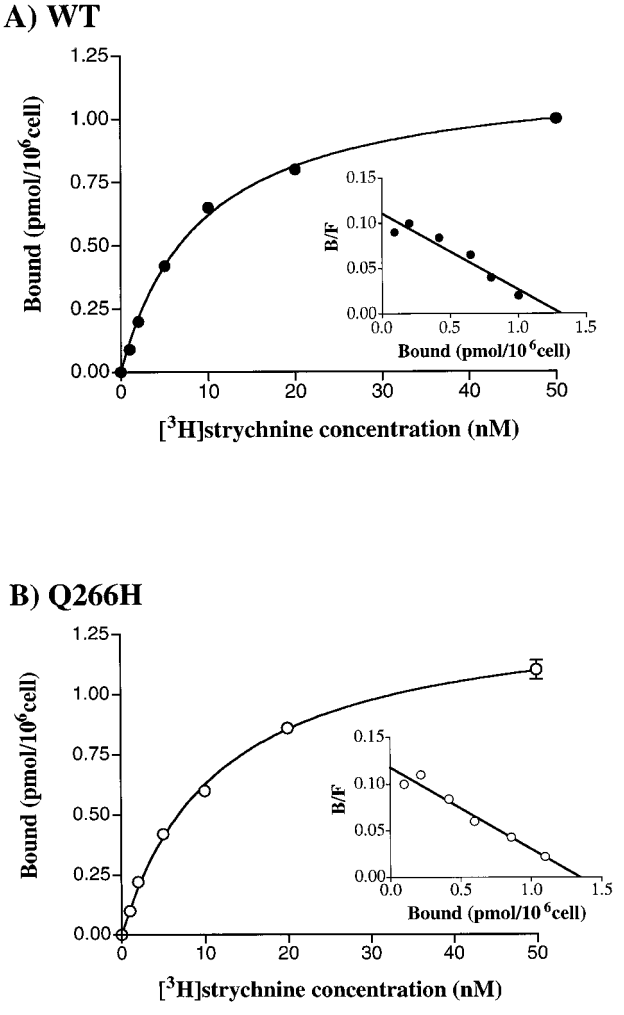

Fig. 3. Saturation isotherm showing specific [3H]strychnine binding to WT (A) and Q266H (B) GlyRs. Scatchard analysis of ligand binding is shown in the inset. The data presented are from one of three independent experiments and show the mean values and S.E.s of triplicate measurements, which are largely obscured by the symbols.

about half of these recordings, both open-time and closed-time histograms had a significantly better fit with the sum of three exponential distributions compared with the sum of two, whereas increasing the number of exponential distributions above three did not significantly improve the fit (see also Twyman and Macdonald, 1991; Takahashi et al., 1992; Lewis et al., 1998). Consequently, to assist comparison between different patches, a three-order exponential equation was imposed to fit all of the distributions. The mean time constants used to describe the dwell times are shown in Tables 2 and 3. There was a general tendency for the three time constants, used to describe the open time of Q266H GlyR single-channel events, to be briefer than those describing the corresponding WT currents, without much change in their relative contributions (Table 2). From the amplitude and relative contribution of each component, overall mean

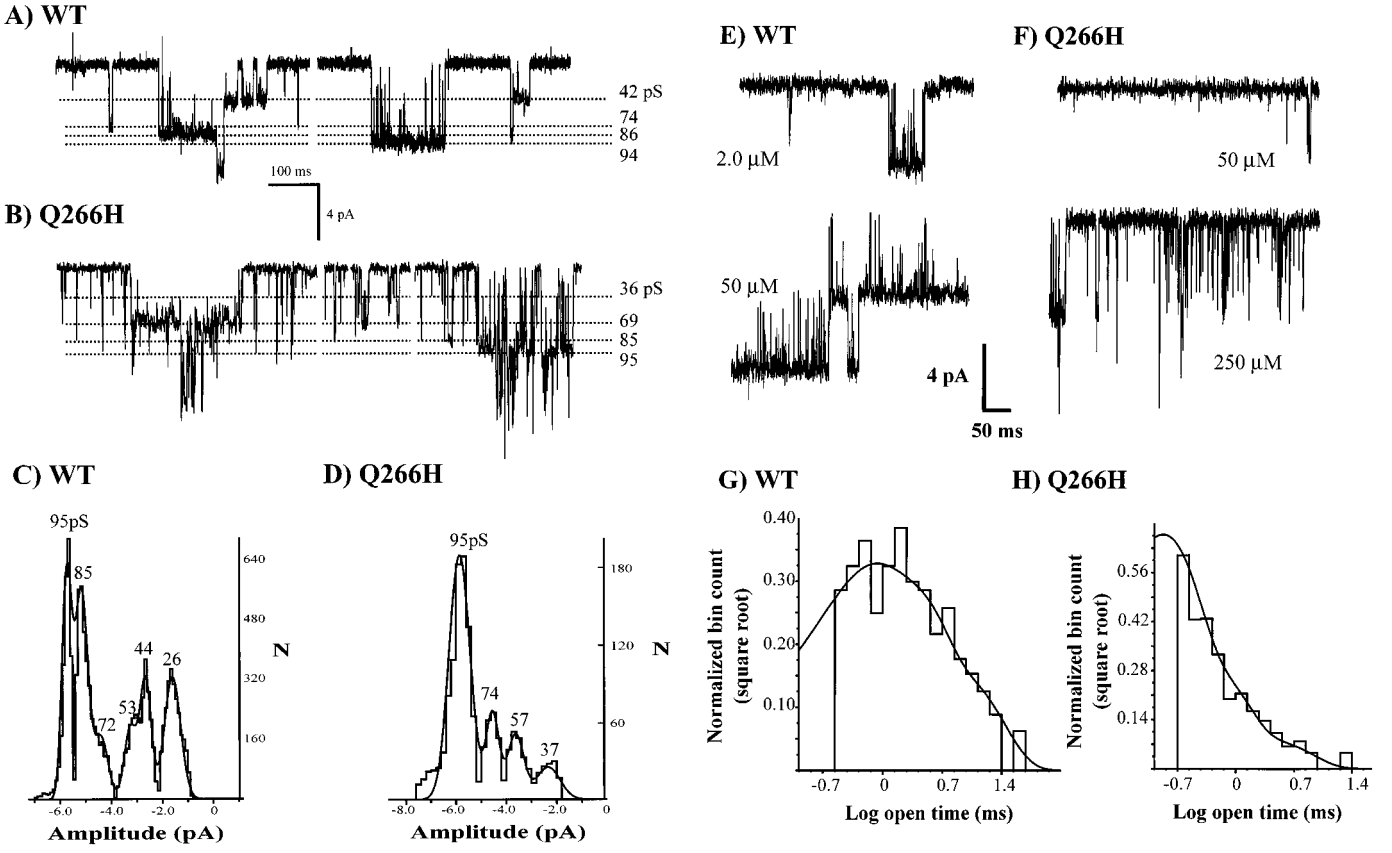

Fig. 4. Examples of single-channel currents and their corresponding amplitude and open-time distributions from separate outside-out patches of WT GlyRs (A, C, E, and G) and Q266H GlyRs (B, D, F, and H) held at −60 mV. A and B, examples of single-channel recordings from WT and Q266H membrane patches, respectively, whereas C and D show their corresponding amplitude histograms. The scale bars refer to both A and B. A and B, data were filtered at 1 kHz and 2 kHz, respectively. Downward deflections indicate inward currents. C and D, the continuous line represents the sum of six and four gaussian distributions, respectively, fit to the histograms. Bin width in C and D was 0.1 and 0.2 pA, respectively. D, an additional peak in the amplitude histogram at about 15 pS has been left out of the histogram for clarity. The scale bar refers to both A and B. E and F, responses to perfusion of both low (upper traces) and higher (lower traces) concentrations of glycine. The scale bar refers to both E and F. It can be seen that the Q266H GlyRs show briefer single-channel events that, at least for those events which could be fully resolved, had a similar amplitude to WT GlyRs. G and H, examples of the open-time distributions of WT and Q266H GlyR single-channel events from the same patch as in E and F, respectively. The fit to these open time histograms with the sum of three exponential distributions are also shown by the continuous curve. C, the time constants and relative proportion of these exponentials were 0.48 ms (37%), 1.88 ms (48%), and 7.95 ms (14%); n = 357 events. D, the time constants and relative proportion of the three exponentials were 0.12 ms (84%); 0.47 ms (15%); and 2.42 ms (1%); n = 479 events.

TABLE 1

Distribution of single-channel conductance levels in WT and Q266H GlyRs

Amplitude and distribution of single-channel conductance states recorded in outside-out membrane patches, excised from HEK-293 cells expressing either α1-homomeric WT or Q266H GlyRs and held at −60 mV in response to low doses of glycine. Eight separate subconductance states were identified. Incidence refers to the number of patches (x) in which the various subconductance states were observed [total number of patches (n) was nine for WT and seven for Q266H GlyRs]. Contribution (%) refers to the mean and S.E.M. of the contribution of that particular conductance state to the total channel activity observed in each patch. The contribution (%) was calculated only from patches in which that particular conductance state was observed.

Conductance Level	I	II	III	IV	V	VI	VII	VIII
WT: − amplitude (pS)	95 ± 0.7	86 ± 1.8	78 ± 0.6	66 ± 2.0	51 ± 1.3	36 ± 1.6	25 ± 0.7	17 ± 0.6
WT: − incidence (x/n)	8/9	3/9	6/9	7/9	5/9	8/9	3/9	4/9
WT: − contribution (%)	39 ± 10	34 ± 4.9	8.8 ± 4.4	23 ± 9.6	17 ± 5.4	15 ± 3.7	15 ± 1.2	7.3 ± 4.4
Q266H: − amplitude (pS)	95 ± 0.9	86 ± 1.0	77 ± 1.7	66 ± 2.6	54 ± 1.2	37 ± 2.1	23 ± 0.5	14
Q266H: − incidence (x/n)	7/7	2/7	5/7	4/7	3/7	4/7	2/7	1/7
Q266H: − contribution (%)	33 ± 10	23 ± 18	24 ± 5.9	23 ± 5.2	17 ± 3.3	28 ± 10	12 ± 8.0	5

open and closed times were calculated. The mean open time for WT single-channel openings was 4.75 ± 0.86 ms (n = 7), whereas that for the Q266H single-channel openings was significantly lower (0.98 ± 0.12 ms, n = 4, p = .02). Unlike the open-time distributions, there was no general tendency for changes in the amplitude or relative contribution of time constants used to describe the distribution of closed times (Table 3). Considering the presence of multiple channels in each patch, it is unclear how these distributions could be interpreted. Suffice it to say that the two briefest components were not altered between the WT and Q266H GlyRs. The longest component of the closed-time distribution was significantly smaller in the Q266H mutants (and this also gave rise to a reduced mean closed time); however, this component is likely to be most sensitive to agonist concentration and the number of channels in the patch (Twyman and Macdonald, 1991; Colquhoun and Hawkes, 1994).

Selectivity and Current Voltage Relationship of GlyRs. Because previous mutagenesis studies on various ion channels have emphasized the importance of residues in the transmembrane region on ion selectivity (Sather et al., 1994), we examined the anion-to-cation selectivity and voltage dependence of whole-cell currents through Q266H GlyRs. In both WT and Q266H GlyRs, glycine elicited an inward current at negative membrane potentials, whereas at positive membrane potentials, the current was outward (Fig. 5, A and B). There was no difference in the reversal potential of these glycine-activated currents, being −0.1 ± 0.4 mV (n = 9) in WT GlyRs and 0.7 ± 0.5 mV (n = 9) in Q266H. Current through the Q266H GlyRs did, however, show what appeared to be some saturation at more extreme potentials, particularly for inward currents (compare Fig. 5, C and D). In cells in which ≥ 90% series resistance compensation was used, and before any current normalization procedure, the linear slope conductance (between +19 mV and −16 mV) was similar in WT (23.5 ± 6.5 nS/pF, n = 8) and in Q266H (21.7 ± 8.7 nS/pF, n = 7) GlyRs.

In a subset of the above experiments, half of the bath NaCl was replaced iso-osmotically with sucrose, to shift the reversal potential for Cl^- currents to a more positive value and determine any changes in Cl^- selectivity. The corresponding current voltage curves are shown in Fig. 5, C and D. There was no difference in the extent of the shift in reversal potential of the glycine-gated current in low NaCl, being 11.3 ± 0.4 mV (n = 4) for WT and 11.0 ± 0.6 mV (n = 4) for Q266H GlyRs, corrected for liquid junction potentials. This indicates that the Q266H mutation does not alter the cation/anion selectivity of the GlyR. The Nernst potential for a perfectly selective Cl^- channel predicted a shift in reversal potential of 14 mV. From the mean shifts in reversal potentials observed, the Goldman-Hodgkin-Katz current equation (correcting for activity coefficients) predicted a Na^+/Cl^- permeability ratio of 0.035 and 0.046 for current through the WT and Q266H receptors, respectively.

For the WT GlyRs in low NaCl, the slope conductance was decreased, particularly for outward currents, as expected from the relationship between single-channel conductance and Cl^- concentration (Bormann et al., 1987; Fatima-Shad and Barry, 1993). For the Q266H GlyRs in low NaCl, however, there was a small increase in slope conductance at positive potentials and an even greater increase at negative potentials. This is particularly evident when a correction is made for the shift in reversal potential (dashed lines in Fig. 5, C and D). Presumably, the Q266H mutation has allowed the channel open probability to be increased by low NaCl.

Effects of pH, Zn^{++}, and DEPC. We took advantage of the introduced histidine residue in the mutant GlyRs and the chemical reactivity of histidine to examine whether residue 266 is exposed to the aqueous channel pore. Histidine reacts with some specificity to Zn^{++} protons and certain protein reagents such as DEPC. In the present experiments, the interpretation of the effects of these reagents was complicated by effects on WT GlyRs. DEPC (≈1 mM) totally abolished the glycine-activated current through both WT GlyRs (n = 2) and Q266H GlyRs (n = 2) (data not shown), making it unsuitable to use as a probe for aqueous exposure of the His266 residue. Zn^{++} has a biphasic effect on the amplitude of glycine-activated currents through native GlyRs and recombinant WT human α1 subunit-containing GlyRs; although some of these complex allosteric effects of Zn^{++} are disrupted in startle disease-mutated GlyRs (Laube et al., 1995a; Lynch et al., 1998). Low concentrations of Zn^{++} (1–10

TABLE 2

Distribution of single-channel open times in WT and Q266H GlyRs

Open-time distribution of the main conductance state in single-channel openings in WT and Q266H GlyRs recorded in outside-out membrane patches held at −60 mV in response to low doses of glycine. The distribution of open times was fitted with three exponential components. τ1, τ2, and τ3 refer to the mean time constants of these exponential components and the percent refers to their relative contribution to the total channel open-time distribution. From the individual time constants and their relative contributions, the mean open time was calculated. All data represent mean and S.E.M. from seven WT and four Q266H GlyR patches. An unpaired t test was used to compare the amplitude and relative contributions of the three components and the mean open time between WT and Q266H. Significant differences ($p < 0.05$) between WT and Q266H are indicated by an asterisk.

Open Times	Mean ± S.E.M.	τ1		τ2		τ3	
	ms	ms	%	ms	%	ms	%
WT	4.75 ± 0.86	0.42 ± 0.19	42 ± 11	2.42 ± 0.76	42 ± 7.3	14.7 ± 3.02	20 ± 3.6
Q266H	0.98 ± 0.12*	0.16 ± 0.09	52 ± 20	0.52 ± 0.17	37 ± 16	3.26 ± 1.13*	12 ± 6.1

TABLE 3

Distribution of single-channel closed times in WT and Q266H GlyRs

Closed-time distribution of the main conductance state in single-channel openings in WT and Q266H GlyRs recorded at −60 mV in response to low doses of glycine. Significant difference ($p < 0.05$) between WT and Q266H is indicated by an asterisk. Data are presented as described in the legend to Table 2.

Closed Times	Mean ± S.E.M.	τ1		τ2		τ3	
	ms	ms	%	ms	%	ms	%
WT	113 ± 35.0	0.40 ± 0.13	38 ± 13	5.92 ± 2.82	21 ± 4.4	185 ± 49.1	41 ± 10
Q266H	37.6 ± 15.2	0.63 ± 0.29	26 ± 2.7	4.31 ± 1.09	25 ± 1.6	32.2 ± 10.1*	50 ± 3.8

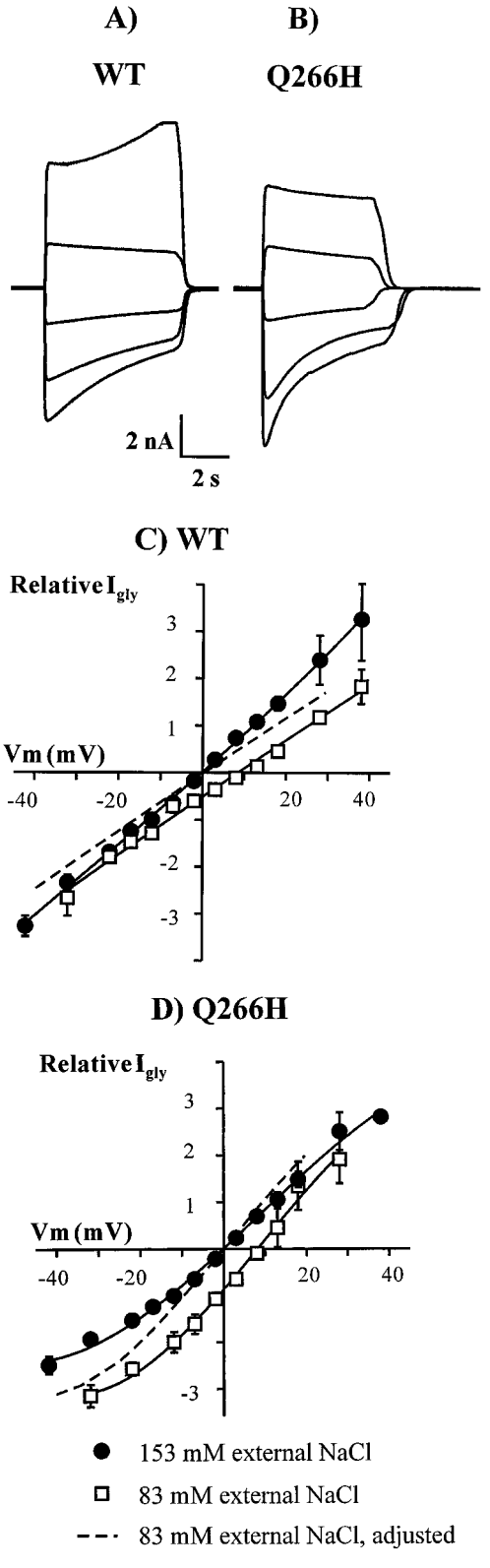

Fig. 5. Voltage dependence of glycine-activated whole-cell currents for WT (A) or Q266H (B) GlyRs in response to supramaximal glycine concentrations (1 and 10 mM respectively). A and B, currents elicited at holding potentials of −21 mV (lower trace), −11 mV, −1 mV, 9 mV, and 19 mV (upper trace) are shown. The slower onset outward current at +19 mV (particularly noticeable in A) was occasionally observed, especially when glycine-activated outward currents were large, and often resulted in swelling and bursting of the cell. The scale bar refers to both A and B. C, current-voltage relationship for glycine-activated currents in cells expressing WT GlyRs bathed in symmetrical 153 mM Cl^- (●) and in an external solution of 83 mM NaCl (□). To normalize current from different experiments, it has been expressed relative to the current observed at a holding potential of 14 mV. The filled circles represent the mean of eight experiments, whereas the open squares represent the mean from a subset of these experiments ($n = 4$). D, current-voltage relationship for glycine activated currents in cells expressing Q266H GlyRs bathed in symmetrical 153 mM Cl^- (●) and in an external solution of 83 mM NaCl (□). Data have been normalized as in C. The filled circles represent the mean of seven experiments, whereas the open squares represent the mean from a subset of these experiments ($n = 4$). C and D, the error bars, representing S.E.M., are shown when larger than the symbols, and the continuous lines are third-order regression fits to the data. The dashed lines in C and D show the current-voltage relationship observed in low external NaCl and corrected for the change in reversal potential (i.e., the curve was redrawn and shifted to the left so that it passed through the origin). This procedure was undertaken so as to more easily compare the slope of the current-voltage relationship in normal and reduced NaCl.

μM) caused an initial enhancement of the glycine (20 μM) activated current through WT GlyRs of about 120%, whereas Zn^{++} concentrations above 10 μM caused a later inhibition of the current (Fig. 6A). In contrast, glycine (150 or 200 μM) activated current through Q266H GlyRs never showed an enhancement in the presence of low Zn^{++} concentrations ($n = 4$). One millimolar Zn^{++} inhibited WT and Q266H GlyRs by a similar degree, inhibiting current through WT GlyRs by 72 ± 9.5% ($n = 3$) and by 88 ± 4.3% ($n = 3$) for Q266H GlyRs, indicating that the mutation did not confer enhanced Zn^{++} sensitivity on the mutant channels. Preliminary concentration-response curves suggested that the IC_{50} for Zn^{++} inhibition of Q266H GlyR current was almost double that for Zn^{++} inhibition of WT GlyR current (Fig. 6B), being about 80 μM for the Q266H GlyRs and about 40 μM for the WT GlyRs. The direction of this shift in the concentration-response curve is opposite to that expected if Zn^{++} reacted with His in the aqueous pore. These results thus provide no evidence that the histidine side chain was exposed to the channel interior, although they do show that the Q266H mutation also impairs the initial allosteric potentiation of current amplitude by low concentrations of Zn^{++} that is seen in WT GlyRs.

The current through both WT and Q266H GlyRs activated by an approximate half-maximal concentration of glycine was reduced, relative to that measured at pH 7.4, at both low pH (6.4) and high pH (8.4) (Fig. 7). The extent of inhibition was similar whether the altered pH solution was applied when the channels were predominantly open or whether it was applied when the channels were closed (i.e., in the presence or absence of glycine, respectively; Fig. 7, A and B). The inhibition was also similar at both negative (−21 mV) and positive (+19 mV) membrane potentials (Fig. 7C), indicating little voltage dependence and suggesting that some allosteric interaction, as opposed to direct channel pore block, mediates the inhibition. At a holding potential of −21 mV, WT GlyR current was decreased by 75 ± 5% ($n = 6$) at pH 6.4 and by 48 ± 8% at pH 8.4 ($n = 6$, $p = .01$). The inhibition of current through Q266H GlyRs induced by changes in pH was significantly less than that observed for WT GlyRs. At a holding potential of −21 mV, Q266H GlyR current was decreased by 33 ± 8% ($n = 5$, $p < .01$) at pH 6.4 and virtually unaffected at pH 8.4 (5 ± 3% inhibition, $n = 5$, $p < .01$). This result is likely to reflect another example of how the Q266H mutation has impaired allosteric modulation by pH rather than reflecting a change in pH sensitivity due to exposure of histidine side chain to the channel interior.

The perfusion of both WT and Q266H transfected HEK-293 cells with a bath solution of pH 6.4 induced an initial transient inward current which inactivated during the ≈8 s perfusion time (Fig. 7A). Although the identity of this current was not investigated, there was no difference in its incidence, amplitude, or time course between WT GlyR and Q266H GlyR-transfected cells.

Discussion

The present study has investigated the functional effects of the Q266H missense mutation of the human GlyR that causes autosomal dominant hyperekplexia, or startle disease. The mutation primarily manifests itself as a 6-fold increase in glycine EC_{50} and a large decrease in single-channel open time without associated major changes in ligand-binding parameters, or permeation properties, such as conductance and anion-to-cation selectivity. There was also a striking difference between WT and Q266H GlyRs in their response to taurine. Taurine was converted from a full agonist at WT GlyRs into a weak partial agonist at Q266H GlyRs, and caused antagonism of the response of the latter GlyRs to the full agonist glycine. This change in agonist behavior has been observed in all of the hyperekplexia mutations studied to date and confirms the notion that this agonist/antagonist behavior is determined by channel-gating efficacy and not ligand binding affinity. All of these observations are consistent with the Q266H mutation causing an impairment of GlyR channel gating.

Comparison with Other Startle Disease Mutations. In previous studies of hyperekplexia mutations, the different mutations have all shown an impaired ability for glycine to activate the channel and the agonist taurine was converted to either a partial agonist or a full antagonist (Laube et al., 1995b; Rajendra et al., 1995; Lynch et al., 1997). The degree

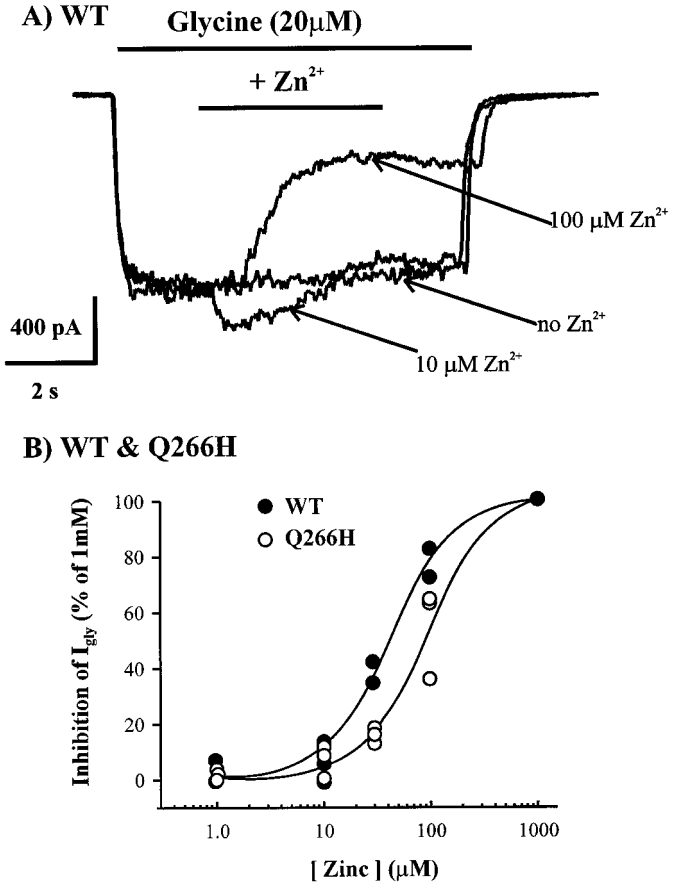

Fig. 6. Actions of $ZnCl_2$ on whole-cell glycine-activated currents in WT and Q266H GlyRs. A, examples of glycine- (10 μM) activated current through WT GlyRs illustrating initial potentiation of current upon coapplication of glycine and low doses of $ZnCl_2$ (10 μM) and a delayed inhibition in response to coapplication of glycine and larger doses of $ZnCl_2$ (100 μM). Holding potential was −21 mV. B, dose-response curves for the Zn^{++}-induced inhibition of glycine-activated currents through WT (closed symbols) and Q266H (open symbols) GlyRs. Points represent individual data points from either two (WT) or three (Q266H) experiments. The lines represent Hill fits to the mean of these data points with EC_{50} and n_H values, respectively, of 34.4 ± 6.0 μM and 1.29 ± 0.25 for the WT and 91.7 ± 3.0 and 1.54 ± 0.07 for the Q266H GlyRs.

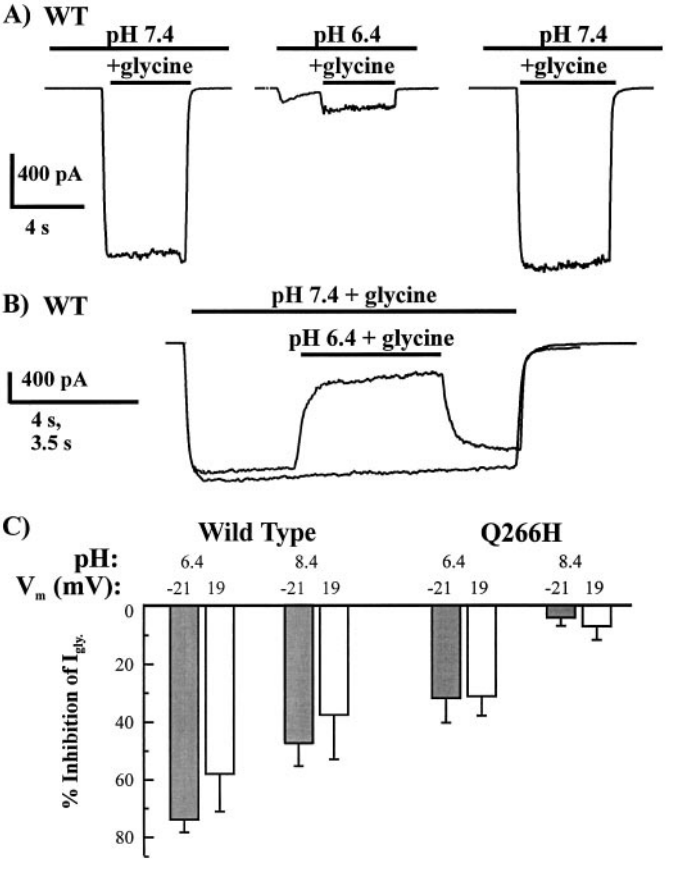

Fig. 7. The effects of changing extracellular pH on glycine-activated whole-cell currents. A, currents through WT GlyRs in response to 20 μM glycine dissolved in the buffered external solution with a pH of 7.4 or 6.4. Note the reversible reduction in glycine-gated current amplitude and the small, transient, inward current produced by perfusing the cell with the reduced pH solution. Holding potential was −21 mV B, two successive glycine-activated currents superimposed. In the first, glycine (20 μM, pH 7.4) is applied continuously for about 10 s, whereas in the second trace, the 10-s application of glycine (20 μM, pH 7.4) is interrupted by a 4-s application of the lower pH glycine solution (20 μM, pH 6.4). The first response, recorded at pH 7.4, has been stretched horizontally for clarity by about 15%. Consequently, the time bar for this trace corresponds to 3.5 s and to 4 s for the subsequent response. This shows that the reduction in current also occurs when the lower pH glycine solution is applied during the application of glycine. Holding potential was −21 mV. C, bar graph showing the extent of inhibition of current through WT and Q266H GlyRs, relative to the current measured at pH 7.4, by both low pH (6.4) and high pH (8.4), at both negative (−21 mV; filled columns) and positive (19 mV; open columns) holding potentials. Bar graphs and error bars represent the mean and S.E.M. of inhibition of glycine-activated current in six (WT) and five (Q266H) separate cells.

of this conversion and the extent of the shift in the concentration response curve has been used to classify the different startle disease mutations as "partial" or "complete" disruption phenotypes (Lynch et al., 1997). The Q266H mutation resembles the partial phenotype because there is a less than 10-fold shift of EC_{50} and taurine can cause some receptor activation and does not totally inhibit glycine-gated currents. Both phenotypes are also associated with abolition of the allosteric potentiation of glycine currents by Zn^{++} (Lynch et al., 1998), an effect also seen for the Q266H mutation. However, the position of the Q266H mutation is quite different to those previously identified; lying within the transmembrane M2 region as opposed to the extracellular M2 to M3 loop or the intracellular M1 to M2 loop. Nevertheless, the phenotypes of all of these startle disease mutations seem to have some qualitatively similar actions. Our results suggest that the transduction mechanism mediating channel opening, agonist/antagonist discrimination, and Zn^{++} potentiation of glycine-gated currents also involves residues in the M2 domain. However, it is still consistent with the M1 to M2 and M2 to M3 loops acting as hinges for movement of the actual channel "gate" in the M2 domain (Lynch et al., 1997). In contrast to this mutation, the two Arg271 mutations, both of which result in the removal of the ring of positive charge at the extracellular border of the M2 domain, cause a radical decrease in the maximum whole cell current response and a decrease in single channel conductance due to a redistribution of subconductance states to lower levels (Langosch et al., 1994; Rajendra et al., 1995). It thus seems that the Arg271 mutations affect ion permeation in addition to gating, implying that the ring of positive charge directly affects conductance. The present study has uncovered a startle disease mutation that has normal single-channel conductance levels, but has impaired channel kinetics. It bears most similarity to the K276E startle disease mutation that has recently been shown to cause a shift in EC_{50}, a decrease in single-channel open time, and a shift in the open-closed equilibrium without any appreciable change in single-channel conductance (Lewis et al., 1998).

Possible Mechanisms Mediating the Effects of the Mutation. EC_{50} depends both on the ligand-binding affinity and efficacy of gating (Colquhoun and Farrant, 1993). The data in this study indicate a clear reduction in channel open times with little change in the briefest closed times, suggesting that the Q266H impairs the efficacy of gating and stabilizes the closed state or destabilizes the open state (see kinetic schemes in Colquhoun and Hawkes, 1994; Aidley and Stanfield, 1996). The lack of change in maximal whole-cell current and n_H for glycine-gated currents in the mutant GlyRs, coupled with the large reduction in the taurine response, suggests that glycine is a high-efficacy agonist at the WT GlyR, whereas taurine is a lower efficacy agonist. Gln266 may play a role in the rotation, or some movement, of the M2 domain that has been suggested to occur on the basis of electron micrographic evidence (Unwin, 1995).

Despite the impairment of channel gating in the Q266H GlyR, it was interesting to note no change in the distribution of subconductance states in the mutant. The most plausible explanation for this is that there is a common or similar mechanism for gating or activation of these subconductance states. A similar conclusion about gating was drawn by Twyman and Macdonald (1991) for two main subconductance states in spinal neurons based on the similarity of their open and burst kinetics.

Relative Position of the Q266H Residue in the Channel Pore. How may the substitution of a glutamine with histidine, an amino acid of similar volume, cause this gating impairment? Could its side chain contribute to a structural component of a "gate"? Exposure of the histidine side chain to the pore interior may have resulted in some change in conduction in response to Zn^{++}, protons, and DEPC (De Biasi et al., 1993; Lu and MacKinnon, 1995). The maximum inhibition by 1 mM Zn^{++} was similar in both receptor types, whereas the sensitivity to Zn^{++} and the inhibition of current at both pH 6.4 and 8.4 was actually reduced in the Q266H mutant. In addition, this inhibition induced by the changes in pH was voltage-independent (Fig. 7). Such voltage-independence for both WT and mutants for the different pH values suggests a site of action outside the membrane field (i.e., not in the channel pore). It seemed unlikely that electrostatic repulsion reduced the access of Zn^{++} (and perhaps also protons) to this outer vestibule region of the pore because in the homologous nAChR and $GABA_A$ receptor channels methanethiosulphonate reagents of the opposite charge to the permeating ion can penetrate the open channel from the extracellular end at least as far as the residue homologous to threonine 265 (i.e., one residue deeper into the pore than the 266 residue) (Xu and Akabas, 1993; Akabas et al., 1994). This suggests that inhibition by Zn^{++} and pH is not mediated by direct actions within the conduction pathway. Indeed, it has recently been shown that the potentiating action of Zn^{++} on recombinant α1-homomeric GlyRs is independent of effects on binding and is mediated instead via allosteric effects on the gating process (Lynch et al., 1998). The above effects of these two agents suggest that the Gln266 residue does not extend its sidechain into the channel interior and does not interact directly with the permeating ion.

Implications for Other LGICs. This study provides the first evidence that residues within the M2 domain of LGICs can impair gating without actually being exposed to the channel interior and without directly interacting with the permeant ion. A number of single-point mutations in the nAChR channel do, however, show a similar relationship between parallel shifts in the whole-cell concentration-response curve and changes in channel open time. In particular, these studies involved mutations to either the conserved leucine residue in the central part of the M2 domain of all LGIC subunits, or in other M2 residues thought to be exposed to the pore, some of which are causative for slow channel congenital myasthenia (Filatov and White, 1995; Engel et al., 1996; Lena and Changeux, 1997). In contrast to these "gain of function" congenital myasthenia mutations which increase channel open time and sensitivity to ligand, the hyperekplexia mutations show an opposite "decrease of function" phenotype.

Physiological Relevance for Inhibitory Neurotransmission and Disease Phenotype. The present study has identified an impairment in the function of GlyR α1-homomeric channels with all five subunits containing the Q266H mutation. Native GlyRs are composed of both α and β subunits (Langosch et al., 1988), and affected individuals for this dominantly inherited disorder are heterozygous. Incorporation of WT α1 subunits and/or β subunits with the mutated α1 subunits would thus be expected to reduce the GlyR

impairments identified in the present study, as has been observed in vitro when combinations of other hyperekplexia mutated α1 subunits and native β subunits have been coexpressed (Langosch et al., 1994; Laube et al., 1995b). That this still leads to the observed phenotype suggests that only minor impairments of the GlyR function are sufficient to impair motor control (see Brune et al., 1996). How may this impairment come about? A number of studies on the developmental changes in glycinergic (Takahashi et al., 1992) or nicotinic (Sakmann and Brenner, 1978; Mishina et al., 1986) transmission have shown a close correlation with the mean open time of single-channel events and the decay time of synaptic currents. Presumably then, individuals with the Q266H mutation will have glycinergic synaptic potentials of reduced duration and amplitude causing impairment of motor control.

Acknowledgments

We thank Kerrie Pierce for constructing the Q266H mutant, Dr. Bill Sewell for the gift of human CD4 cDNA, and Sharon Fielder and Irene Michas for excellent technical assistance. We also thank Dr. Joe Lynch for initial comments and suggestions and Dr. Trevor Lewis for helpful comments on the manuscript.

References

Aidley DJ and Stanfield PR (1996) *Ion Channels: Molecules in Motion*, pp 161–174, University Press, Cambridge.

Akabas MH, Kaufmann C, Archdeacon P and Karlin A (1994) Identification of acetylcholine receptor channel-lining residues in the entire M2 segment of the α subunit. *Neuron* **13:**919–927.

Barry PH (1994) JPCalc: A software package for calculating liquid junction potential corrections in patch-clamp, intracellular, epithelial and bilayer measurements and for correcting junction potential measurements. *J Neurosci Methods* **51:**107–116.

Bertrand D, Galzi J-L, Devillers-Thiéry A, Bertrand S and Changeux JP (1993) Stratification of the channel domain in neurotransmitter receptors. *Curr Opin Cell Biol* **5:**688–693.

Bormann J, Hamill OP and Sakmann B (1987) Mechanism of anion permeation through channels gated by glycine and γ-aminobutyric acid in mouse cultured spinal neurons. *J Physiol (London)* **385:**243–286.

Brune W, Weber RG, Saul B, von Knebel Doeberitz M, Grond-Ginsbach C, Kellermann K, Meinck H-M and Becker C-M (1996) A GLRA1 null mutation in recessive hyperekplexia challenges the functional role of glycine receptors. *Am J Hum Genet* **58:**989–997.

Chen C and Okayama H (1987) High efficiency expression of mammalian cells by plasmid DNA. *Mol Cell Biol* **7:**2745–2751.

Colquhoun D and Farrant M (1993) The binding issue. *Nature (London)* **366:**510–511

Colquhoun D and Hawkes AG (1994) The interpretation of single channel recordings, in *Microelectrode Techniques,* (Ogden DC ed) 2nd ed pp 141–188, The Company of Biologists Limited, Cambridge.

De Biasi M, Drewew JA, Kirsch GE and Brown AM (1993) Histidine substitution identifies a surface position and confers Cs^+ selectivity on a K^+ pore. *Biophys J* **65:**1235–1242.

Elmslie FV, Hutchings SM, Spencer V, Curtis A, Covanis T, Gardiner RM and Rees M (1996) Analysis of GLRA1 in hereditary and sporadic hyperekplexia: a novel mutation in a family co-segregating for hyperekplexia and spastic paraparesis. *J Med Genet* **33:**435–436.

Engel AG, Ohno K, Milone M, Wang H-L, Nakano S, Bouzat C, Pruit II JN, Hutchinson DO, Brengman JM, Bren N, Sieb JP and Sine SM (1996) New mutations in acetylcholine receptor subunit genes reveal heterogeneity in the slow-channel congenital myasthenic syndrome. *Hum Mol Genetics* **5:**1217–1227.

Fatima-Shad K and Barry PH (1993) Anion permeation in GABA- and glycine-gated channels of mammalian cultured hippocampal neurons. *Proc R Soc Lond B Biol Sci* **253:**69–75.

Filatov GN and White MM (1995) The role of conserved leucines in the M2 domain of the acetylcholine receptor in channel gating. *Mol Pharmacol* **48:**379–384.

Floeter MK and Hallet M (1993) Glycine receptors: A startling connection. *Nat Genet* **5:**319–320.

Langosch D, Thomas L. and Betz H (1988) Conserved quaternary structure of ligand-gated ion channels: The postsynaptic glycine receptor is a pentamer. *Proc Natl Acad Sci USA* **85:**7394–7398.

Langosch D, Laube B, Rundström N, Schmeiden V, Bormann J and Betz H (1994) Decreased agonist affinity and chloride conductance of mutant glycine receptors associated with human hereditary hyperekplexia. *EMBO J* **13:**4223–4228.

Laube B, Kuhse J, Rundström N, Kirsch J, Schmieden V and Betz H (1995a) Modulation by zinc ions of native rat and recombinant human inhibitory glycine receptors. *J Physiol (London)* **483.3:**613–619.

Laube B, Langosch D, Betz H and Schmieden V (1995b) Hyperekplexia mutations of the glycine receptor unmask the inhibitory subsite for β-amino-acids. *NeuroReport* **6:**897–900.

Lena C and Changeux J-P (1997) Pathological mutations of nicotinic receptors and nicotine-based therapies for brain disorders. *Curr Opin Neurobiol* **7:**674–682.

Lewis TM, Sivilotti LG, Colquhoun D, Gardiner RM, Schoepfer R and Rees M (1998) Properties of human glycine receptors containing the hyperekplexia mutation α1(K276E), expressed in *Xenopus* oocytes. *J Physiol (London)* **507.1:**25–40.

Lu Z and MacKinnon R (1995) Probing a potassium channel pore with an engineered protonatable site. *Biochemistry* **34:**13133–13138.

Lynch JW, Rajendra S, Barry PH and Schofield PR (1995) Mutations affecting the glycine receptor agonist transduction mechanism convert the competitive antagonist, picrotoxin, into an allosteric potentiator. *J Biol Chem* **270:**13799–13806.

Lynch JW, Rajendra S, Pierce KD, Handford CA, Barry PH and Schofield PR (1997) Identification of intracellular and extracellular domains mediating signal transduction in the inhibitory glycine receptor channel. *EMBO J* **16:**110–120.

Lynch JW, Jacques P, Pierce KD and Schofield PR (1998) Zinc potentiation of the glycine receptor chloride channel is mediated by allosteric pathways. *J Neurochem* **71:**2159–2168.

Milani N, Dalpra L, Delprete A, Zanini R and Larizza L (1996) A novel mutation (Gln266→His) in the alpha1 subunit of the inhibitory glycine-receptor gene (GLAR1) in hereditary hyperekplexia. *Am J Hum Genet* **58:**420–422.

Mishina M, Takai T, Imoto K, Noda M, Takahashi T, Numa S, Methfessel C and Sakmann B (1986) Molecular distinction between fetal and adult forms of muscle acetylcholine receptor. *Nature (London)* **321:**406–411.

Rajendra S, Lynch JW, Pierce KD, French CR, Barry, PH and Schofield PR (1994) Startle disease mutations reduce the agonist sensitivity of the human inhibitory glycine receptor. *J Biol Chem* **269:**18739–18742.

Rajendra S, Lynch JW, Pierce KD, French CR, Barry, PH and Schofield PR (1995) Mutation of a single amino acid in the human glycine receptor transforms β-alanine and taurine from agonists into competitive antagonists. *Neuron* **14:**169–175.

Rees MI, Andrew M, Jawad S and Owen MJ (1994) Evidence for recessive as well as dominant forms of startle disease (hyperekplexia) caused by mutations in the α subunit gene of the inhibitory glycine receptor. *Hum Mol Genet* **3:**2175–2179.

Sakmann B and Brenner HR (1978) Changes in synaptic channel gating during neuromuscular development. *Nature (London)* **276:**401–402.

Sather WA, Yang J and Tsien RW (1994) Structural basis of ion channel permeation and selectivity. *Curr Opin Neurobiol* **4:**313–323.

Schofield PR, Lynch JW, Rajendra S, Pierce KA, Handford CA and Barry PH (1996) Molecular and genetic insights into ligand binding and signal transduction at the inhibitory glycine receptor. Cold Spring Harbor Symp Quant Biol **61:**333–342.

Shiang R, Ryan SG, Zhu Y-Z, Hahn AF, O'Connell P and Wasmuth JJ (1993) Mutations in the α1 subunit of inhibitory glycine receptor causing the dominant neurological disorder, hyperekplexia. *Nature Genet* **5:**351–358.

Shiang R, Ryan SG, Zhu Y-Z, Fielder TJ, Allen RJ, Fryer A, Yamashita S, O'Connell P and Wasmuth JJ (1995) Mutational analysis of familial and sporadic hyperekplexia. *Ann Neurol* **38:**85–91.

Takahashi T, Momiyama A, Hirai K, Hishinuma F and Akagi H (1992) Functional correlation of fetal and adult forms of glycine receptors with developmental changes in inhibitory synaptic receptor channels. *Neuron* **9:**1155–1161.

Twyman RE and Macdonald RL (1991) Kinetic properties of the glycine receptor main- and sub-conductance states of mouse spinal cord neurones in culture. *J Physiol (London)* **435:**303–331.

Unwin N (1995) Acetylcholine receptor imaged in the open state. *Nature (London)* **359:**37–43.

Xu M and Akabas MH (1993) Amino acids lining the channel of the γ-aminobutyric acid type A receptor identified by cysteine substitution. *J Biol Chem* **29:**21505–21508.

Zafra F, Aragón C and Giménez C (1997) Molecular biology of glycinergic neurotransmission. *Mol Neurobiol* **14:**117–142.

Send reprint requests to: Dr. Peter H. Barry, School of Physiology and Pharmacology, University of New South Wales, Sydney, 2052, Australia. E-mail: p.barry@unsw.edu.au